FULL PAPER

Dalton
www.rsc.org/dalton

The coordination chemistry of 1,2,4-triazinyl bipyridines with lanthanide(III) elements – implications for the partitioning of americium(III)

Michael J. Hudson,*[a] Michael G. B. Drew,[a] Mark R. StJ. Foreman,[a] Clément Hill,[b] Nathalie Huet,[a] Charles Madic[b] and Tristan G. A. Youngs[a]

[a] *Department of Chemistry, University of Reading, Box 224, Whiteknights, Reading, UK RG6 6AD. E-mail: m.j.hudson@reading.ac.uk*

[b] *Commissariat d'Energie Atomique, DEN/bat 400, CEA-Valrho (Marcoule), B.P. 17171 Bagnol-sur Cèze, Cédex France*

Received 29th January 2003, Accepted 25th March 2003
First published as an Advance Article on the web 7th April 2003

It has been established that 6-(5,6-dialkyl-1,2,4-triazin-3-yl)-2,2′-bipyridines (*R,hemi-BTPs*) have properties which are intermediate between those of the terpyridines and the bis(1,2,4-triazin-3-yl)pyridines (BTPs). However, they resemble the terpyridines much more closely than the BTPs. It has been shown that *Et,hemi-BTP* when dissolved in TPH—a dodecane-like solvent—is a selective reagent for the separation of americium(III) from europium(III). Solution NMR in acetonitrile largely confirmed the crystallographic results. There was no evidence for a 1 : 3 complex cation, or for significant differences between metal(III)–N distances for the pyridine and 1,2,4-triazine rings. Intramolecular hydrogen bonding plays a crucial role in the formation of metal coordination spheres, which explains the differences between the terpyridyl, *R,hemi-BTPs* and the BTPs. Protonation of the *R,hemi-BTPs* facilitates a conformational change which is necessary for complexation.

Introduction

The partitioning of minor actinides(III) from lanthanides(III) remains an important problem in the management of nuclear waste. Much attention has been focussed on nitrogen heterocyclic molecules since it is possible, in principle, to use these reagents to separate the minor actinides such as americium(III) from europium(III) in the aqueous PUREX raffinate.[1] There have been extensive investigations into the f-block coordination chemistry of ligands such as terpyridine (**1**) and the bis(1,2,4-triazin-3-yl)pyridines (BTPs, **2**), Fig. 1. It is surprising, however, that despite their utility as synthetic intermediates[2] that so little work has been conducted on 6-(5,6-dialkyl-1,2,4-triazin-3-yl)-2,2′-bipyridines (*R,hemi-BTPs*), such as molecules (**3**) and (**4**) in Fig. 1, which are derivatives of bipyridyl with bound 1,2,4-triazine groups.[3] Although it has been shown that triazin-3-yl oligopyridines are able to bind to iron[4] and ruthenium,[5] no studies have been reported on the coordination chemistry of these reagents with f-block elements. Combined parallel synthesis and analysis of selected N-heterocycles clearly indicated that 6-(5,6-dialkyl-1,2,4-triazine-3-yl)-2,2′-bipyridines shown as (**3**) and (**4**) in Fig. 1, are potential reagents for the partitioning of minor actinides.[6] Consequently, this study is the first detailed investigation into the coordination chemistry of these reagents with f-block elements.

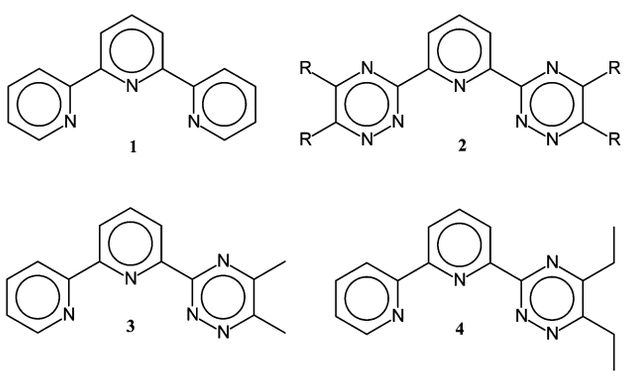

Fig. 1 Terpyridine (**1**); bis-2,6-(1,2,4-triazine-3-yl)pyridines (**2**) – a BTP; 6-(5,6-dimethyl-1,2,4-triazin-3-yl)-2,2′-bipyridine (**3**) (*Me,hemi-BTP*); 6-(5,6-diethyl-1,2,4-triazin-3-yl)-2,2′-bipyridine (**4**) (*Et,hemi-BTP*).

It is known that hydrophobic reagents derived from terpyridine (**1**), when dissolved in dodecane-like solvents, in synergistic combination with α-substituted carboxylic acids such as α-bromodecanoic acid, possess a moderate extraction selectivity ($SF_{Am/Eu} = 7$ from dilute nitric acid) for americium(III) over europium(III).[7] Terpyridine forms mononuclear lanthanide complexes that contain one or two ligands.[8,9] In addition to forming lanthanum complexes, **1** after protonation is able to act as part of a large planar counter ion, which enables $[La(NO_3)_6]^{3-}$ to co-crystallize. Mononuclear lanthanum nitrate complexes in which the metal to organic ligand ratio is 1 : 1 are known of 2,6-bis-(5-methyl-1*H*-[1,2,4]triazol-3-yl)pyridine,[10] and terpyridine (**1**).[11] The maintenance of the coordination number of the metal by the alternation of two water molecules for a nitrate anion in a coordination sphere is a common feature of the structural chemistry of lanthanide nitrate complexes.[12] Lanthanum nitrate, in common with the yttrium and praesodymium nitrates, forms a mononuclear neutral hydrated complex with 4,6-bis(pyridin-2-yl)-1,3,5-triazin-2-ylamine.[13] Gadolinium and erbium nitrates form hydrated mononuclear cationic complexes with 4,6-bis(pyridin-2-yl)-1,3,5-triazin-2-ylamine. Neodymium(III) is able to form both neutral trinitrate and cationic dinitrate complexes with 4,6-bis(pyridin-2-yl)-1,3,5-triazin-2-ylamine. When a large poorly coordinating anion such as $[La(NO_3)_4(terpy)]^-$ is present, two neutral **1** ligands and two nitrates bind to a lanthanum centre within the $[La(NO_3)_2(terpy)_2]^+$ cation.[14] When the nitrate ligands have been replaced with the less coordinating perchlorate anions, three molecules of terpyridine can bind to a lanthanum centre. The reaction of lanthanum(III) bromide with **1** results in the formation of a hydrated tricationic complex.[15] Carboxylate ligands can bridge between lanthanum centres in the dinuclear trichloroacetate $[La_2(Cl_3COO)_6(terpy)_2]$,[16] which is similar to the structure obtained by reacting *Me,hemi-BTP* with lanthanum nitrate. It is rare, however, for terpyridine to form nitrato-complexes in which there are three terpyridine ligands.[17] Indeed, it is thought that one of the reasons why the terpyridine

DOI: 10.1039/b301178j

reagents only give modest separation factors is because the coordination sphere of the metal(III) cation is not completely enclosed by the nitrogen heterocycle, and also contains nitrate and water molecules with the result that it is difficult to form a single hydrophobic species.[18] The bis(triazinyl)pyridine (BTP) class of ligands (**2**) often have far greater selectivites ($SF_{Am/Eu}$ > 20) than terpyridine.[19,20] These greater selectivities have been related to the fact that the BTPs are able to form single hydrophobic species $[Ln(BTP)_3]^{3+}$ in which three BTP ligands completely fill the primary coordination sphere of the metal(III).[21] In such a species it is difficult for water and nitrate ligands to be located within the coordination sphere of the metal cation so that a single hydrophobic entity may be involved in the separation process. It has been shown in a $[Ln(^iPr_4BTP)_3]I_3$ complex that the BTP moiety binds more tightly to f-block metals than does terpyridine in an analogous complex.[22,23] It appears, however, that the BTP reagents are rather unstable against chemical attack and radiolysis.[24]

Consequently, it was decided to investigate the 6-(5,6-dialkyl-1,2,4-triazin-3-yl)-2,2′-bipyridines (*R,hemi-BTPs*), in order to establish whether the chemical properties such as the $SF_{Am/Eu}$ values were similar to those of the terpyridines or to the BTPs. In addition, there was interest in establishing whether there was any evidence for the formation of a 1 : 3 complex as has been confirmed with the BTPs and in establishing any differences or similarities between the pyridine and the triazine rings within the *R,hemi-BTPs.* Attention was directed towards the evaluation of any differences in metal–nitrogen distances that could be detected between the pyridine and triazine rings.

Experimental

^1H, ^{13}C-{^1H} and ^{13}C NMR spectra were recorded using either a Bruker AMX400 or an Avance DPX250 instrument. Chemical shifts are reported in parts per million downfield from tetramethylsilane. All organic reagents were purchased from Acros or Aldrich, while inorganic reagents were obtained from either BDH or Aldrich. 2,2′-Bipyridyl *N*-oxide was obtained by the reaction of 2,2′-bipyridyl with hydrogen peroxide in acetic acid,[25] while 2,2′-bipyridinyl-6-carbonitrile was obtained by the reaction of 2,2′-bipyridyl *N*-oxide with trimethylsilyl cyanide and dimethyl carbamyl chloride in dichloromethane.[26] **WARNING**: trimethylsilyl cyanide is a volatile hydrogen cyanide equivalent. As shown in Fig. 2, the 2,2′-bipyridinyl-6-carbonitrile was converted to 2,2′-bipyridyl-6-carbamidrazone by the action of hydrazine (−hydrate at 30 °C).[27]

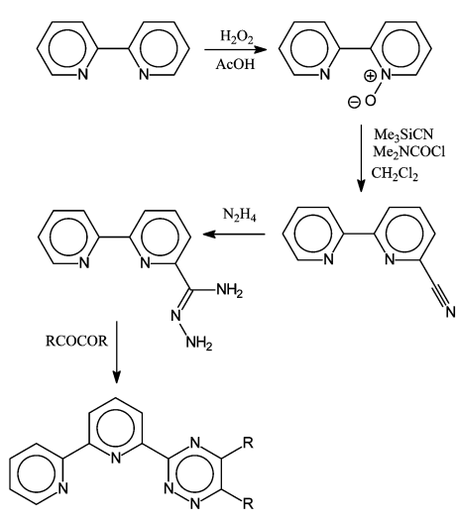

Fig. 2 Overall scheme for the synthesis of the 6-(5,6-dialkyl-1,2,4-triazin-3-yl)-2,2′-bipyridines (*Me,hemi-BTP*) and (*Et,hem-iBTP*).

Table 1 Elemental analyses for the lanthanide complexes of *Me,hemi-BTP*

		Found (%)			Required (%)		
M	Formula	C	H	N	C	H	N
La	$La_2(NO_3)_6(H_2O)_2L_2$	31.2	2.3	19.1	30.6	2.2	19.1
Ce	$Ce_2(NO_3)_6(H_2O)_2L_2$	31.0	2.3	19.0	30.6	2.2	19.0
Nd	$Nd_2(NO_3)_6L_2$	30.8	2.3	18.9	30.4	2.2	18.9
Pr	$Pr(NO_3)_3(H_2O)L$	31.0	2.3	18.9	30.5	2.2	19.0
Gd	$Gd(NO_3)_3(H_2O)_3L$	29.9	2.2	18.1	29.7	2.2	18.5

6-(5,6-Dimethyl-1,2,4-triazin-3-yl)-2,2′-bipyridine (*Me,hemi-BTP*)[28]

A solution of 2,2′-bipyridyl-6-carbamidrazone (2.96 g, 13.9 mmol) and butane-1,2-dione (5 mL, 4.9 g, 57 mmol) in THF (90 mL) was heated (66 °C, 3 h). After cooling the reaction mixture was concentrated by evaporation. The residue was dissolved in dichloromethane (100 mL), and the resulting solution was then washed with brine (10 mL) before being dried (Na_2SO_4). After filtration and removal of solvent under vacuum the solid (3.76 g) was recrystallised from ethanol to give a yellow solid (1.92 g), which was subject to chromatography on silica. The column was initially eluted with dichloromethane, then with 10% ethyl acetate in dichloromethane and finally with 10% ethanol in dichloromethane. After removal of non-polar impurities from the column an orange solid (1.71 g, 47% yield) was obtained. δ_H 8.64 (1H, m), 8.59 (1H, m), 8.52 (1H, m), 8.49 (1H, m), 7.96 (1H, dd, J = 7.9 and 7.9 Hz), 7.79 (1H, m), 7.27 (1H, m), 2.72 (3H, s) and 2.64 (3H, s). MS (CI) 264 (MH^+) and 182 ($C_{11}H_8N_3^+$) *m*/*q*.

6-(5,6-Diethyl-1,2,4-triazin-3-yl)-2,2′-bipyridine (*Et,hemi-BTP*)

A solution of 2,2′-bipyridyl-6-carbamidrazone (507 mg, 2.38 mmol) and hexane-3,4-dione (1 mL, 0.94 g, 8.23 mmol) in THF (20 mL) was heated (66 °C, 4 h). After cooling, the reaction mixture was concentrated by evaporation of the THF. The residue was washed with hexane before being dissolved in dichloromethane (50 mL), and the resulting solution was then washed with brine (10 mL) before being dried (Na_2SO_4). After filtration and removal of solvent in vacuum a yellow solid (665 mg, 96% yield) was obtained. Found: C, 69.6; H, 5.8; N, 23.4%; $C_{17}H_{17}N_5$ requires C, 70.0; H, 5.9; N, 24.0%. δ_H 8.73 (2H, m), 8.59 (2H, m), 8.05 (1H, dd, J = 7.9 and 7.9 Hz), 7.88 (1H, m), 7.36 (1H, m), 3.13 (2H, q, J = 7.5 Hz), 3.00 (2H, q, J = 7.4 Hz) and 1.50 (6H, m). δ_C 162.79 (quat), 161.76 (quat), 160.61 (quat), 156.90 (quat), 156.22 (quat), 153.22 (quat), 149.44, 138.34, 137.39, 124.39, 124.17, 122.78, 122.17, 27.49 (CH_2), 26.10 (CH_2), 12.69 and 11.59. MS (CI) 292 (MH^+) and 182 ($C_{11}H_8N_3^+$) *m*/*q*. Molecular ion found at 292.1574 amu, $C_{17}H_{18}N_5$ requires 292.1562 amu.

Crystals of lanthanide and yttrium complexes of *Me,hemi-BTP*

Dilute acetonitrile solutions of *Me,hemi-BTP* and the metal nitrate were combined, and the resulting mixture was allowed to stand undisturbed for several days. The product was then collected by filtration, washed with acetonitrile and dried in air. In each sample, there was a small loss of water prior to the elemental analysis (see Table 1).

The stability test on *Et,hemi-BTP* in nitric acid

A solution of *Et,hemi-BTP* (36.5 mg) in toluene (12.5 mL) was stirred with nitric acid (12.5 mL of 3 mol dm^{-3}). The aqueous layer changed rapidly from colourless to yellow/brown. On stirring (24 h) no further colour change was observed. The toluene layer was separated from the aqueous layer, which was washed with diethyl ether (10 mL). On evaporation, the toluene and ether layers yielded no residue. Excess sodium hydroxide was added to the aqueous layer, which was extracted with dichloro-

Table 2 The distribution coefficients and separation factors ($SF_{Am/Eu}$) as a function of the nitric acid concentration for *ethyl,hemi-BTP* (0.1 mol dm^{-3}), see Fig. 3

$[HNO_3]_{ini}$/mol L^{-1}	0.021	0.042	0.060	0.099
$A(Eu^{152})_{ini}$/kBq L^{-1}	9766	9697	8182	7909
$A(Eu^{152})_{eq.\ aq.}$/kBq L^{-1}	1900	6760	7210	7820
$A(Eu^{152})_{eq.\ org.}$/kBq L^{-1}	7455	2890	955	185
Activity balance (%)[a]	4%	0%	0%	−1%
D_{Eu}	***3.9***	***4.3 10^{-1}***	***1.3 10^{-1}***	***2.4 10^{-2}***
$A(Am^{241})_{ini}$ /kBq L^{-1}	6924	6835	10720	11140
$A(Am^{241})_{eq.\ aq.}$/kBq L^{-1}	60	525	1990	6270
$A(Am^{241})_{eq.\ org.}$/kBq L^{-1}	6125	5890	7860	4255
Activity balance (%)	11%	6%	8%	6%
D_{Am}	***102***	***11***	***3.9***	***6.8 10^{-1}***
$SF_{Am/Eu}$	***26***	***26***	***30***	***29***
$[HNO_3]$eq/mol L^{-1}	***0.020***	***0.039***	***0.059***	***0.095***

Ini = initial; eq = equilibrium; aq = aqueous and org = organic phase. [a] Difference (initial − final).

Table 3 The distribution coefficients D_{Am} and D_{Eu}, and separation factors ($SF_{Am/Eu}$) as a function of the nitric acid concentration for *ethyl,hemi-BTP* (0.02 mol dm^{-3}) at 25 °C, see Fig. 3

$[HNO_3]_{ini}$/mol L^{-1}	0.021	0.042	0.060	0.080	0.099
$A(Eu^{152})_{ini}$/KBq L^{-1}	9766	9697	8182	8203	7909
$A(Eu^{152})_{eq.\ aq.}$/KBq L^{-1}	4531	8672	8119	8260	7942
$A(Eu^{152})_{eq.\ org.}$/KBq L^{-1}	5388	1096	233	95	41
Activity balance (%)	−2%	−1%	−2%	−2%	−1%
D_{Eu}	***1.2***	***0.13***	***0.029***	***0.012***	***0.0052***
$A(Am^{241})_{ini}$/KBq L^{-1}	6924	6835	10720	11000	11140
$A(Am^{241})_{eq.\ aq.}$/KBq L^{-1}	5388	1096	233	95	41
$A(Am^{241})_{eq.\ org.}$/KBq L^{-1}	6370	4672	3762	1888	955
Activity balance (%)	3%	0%	−1%	−1%	0%
D_{Am}	***20.2***	***2.2***	***0.5***	***0.2***	***0.094***
$SF_{Am/Eu}$	***17***	***17***	***19***	***18***	***18***
$[HNO_3]_{eq}$/mol L^{-1}	***0.022***	***0.042***	***0.062***	***0.082***	***0.100***

Ini = initial; eq = equilibrium; aq = aqueous and org = organic phase.

methane (4 × 5 mL). These dichloromethane extracts were combined, dried (Na_2SO_4), filtered and evaporated to give a yellow solid (32 mg) the NMR spectra (^1H and ^{13}C-{^1H}) of which were identical with those of *Et,hemi-BTP*. See Tables 2 and 3 for further information.

The stability tests performed on *Et,hemi-BTP* in mixed nitric and nitrous acids

Et,hemi-BTP (36 mg) was added to nitric acid (10 mL of 3 mol dm^{-3}), and to the resulting solution was added sodium nitrite (132 mg). The mixture was then left inside a sealed tube. Ten hours later more sodium nitrite (180 mg) was added, and the vial was resealed. After standing for 14 h the vial was opened and the contents treated with sodium hydroxide (10 mL of a 20% solution). No precipitation was observed during the treatment with sodium hydroxide. The mixture was extracted with dichloromethane (4 × 5 mL), and the extracts were combined and evaporated to furnish a white solid (1 mg). The following peaks, which arose from the decomposition products, were observed: MS (CI) 200.0832, 182.0725 and 156.0717 amu.

Radiochemical studies

The aqueous solutions were prepared by spiking dilute nitric acid (concentration between 0.1 and 0.01 mol dm^{-3}) with stock solutions of ^{152}Eu and ^{241}Am (4 GBq dm^{-3}) in nitric acid. The desired initial activity concentration of the aqueous solutions used was approximately 7 to 11 MBq dm^{-3} for each radionuclide (^{152}Eu and ^{241}Am). Solutions of *Et,hemi-BTP* (0.1 and 0.02 mol dm^{-3}) were prepared by dissolving *Et,hemi-BTP* in a solution of 2-bromodecanoic acid (1 mol dm^{-3}) in TPH (a dodecane-like solvent). Each organic phase (700 μL) was shaken separately with each of the aqueous phases in a total of nine extraction experiments for one hour at 25 °C. After mixing with a vortex IKA (Vibrax VXR), and after phase disengagement by centrifugation the phases were separated for radiometric gamma analyses. A CAMBERRA-EURISYS pure Germanium co-axial detector (type P) was employed. The activity balance was always maintained within 10%, and was checked by counting both initial and final aqueous layers and final organic-layers. The acidities of the initial and final aqueous solutions were determined by potentiometric titration against sodium hydroxide solution (0.1 mol dm^{-3}) using a Metrohm 751 GPD Titrino device.

Crystallography

X-Ray diffraction data for all eight crystals were collected with Mo-Kα radiation using the MAR research Image Plate System. Details are provided for the complexes in Table 4. The crystals were positioned 70 mm from the image plate. Ninety five frames were measured at 2° intervals with a counting time of 2 min or less where appropriate. Data analysis was carried out with the XDS program.[29] Structures were solved using direct methods with the Shelx86 program.[30] Non-hydrogen atoms were refined with anisotropic thermal parameters. The hydrogen atoms bonded to carbon were included in geometric positions and given thermal parameters equivalent to 1.2 times those of the atom to which they were attached. In most structures the hydrogen atoms bonded to water molecules could not be located. Empirical absorption corrections were carried out on all structures using the DIFABS program.[31] Two structures in particular involving Ce and Pr metals gave high residual electron density close to the metal position. Structures were refined on F^2 until convergence using Shelxl.[32]

CCDC reference numbers 202727–202734.

See http://www.rsc.org/suppdata/dt/b3/b301178j/ for crystallographic data in CIF or other electronic format.

Results and discussion

Solvent extraction

The solvent extraction studies were carried out in the presence of 2-bromodecanoic acid (*αBrCapH*) since both of the *hemi-BTP* reagents require a synergist to extract americium or europium. In the case of 2-bromodecanoic acid, the reagent is thought to act both as a phase transfer reagent as well as being directly involved in the overall mechanism of the reaction, eqn. (1).

$$n[R,hemi\text{-}BTP] + 3[\alpha BrCapH] + Am(III) = [Am[\alpha BrCap^-]_3(R,hemi\text{-}BTP)_n] + 3H^+ \quad (1)$$

The distribution ratios and the separation factors for *Et,hemi-BTP* are shown in Fig. 3. It can be seen that distribution coefficients for americium(III) are uniformly greater than the corresponding values for europium(III) with a maximum value for D_{Am} of 100. The gradient, which will be discussed later, clearly has a value of −3, which indicates that the acidity of the medium plays a key role in the mechanism of the separation. The corresponding $SF_{Am/Eu}$ values of 28(±2) are constant over the range of acidities. When the concentration of *Et,hemi-BTP* was increased five-fold, the extractions of europium and americium were increased by factors of 3.0 and 4.7, respectively, suggesting that the extracted species has a metal to *Et,hemi-BTP* ratio of up to 1 : 1.

The mechanism of the extraction using the *R,hemi-BTPs* is identical to that for terpyridyl and related molecules but not that of the BTP molecules. The extraction of americium and europium is dependent on the acidity of the solution. Clearly, the optimum D_{Am} was obtained at low acidities. However, the equilibrium does suggest that it will be possible to extract americium(III) at low acidities and strip the metal from the

Table 4 Details of the crystal structures

Structure	$[La_2(NO_3)_6L_2\cdot(H_2O)_2]$	$[Ce_2(NO_3)_6L_2\cdot(H_2O)_2]$	$[Pr(NO_3)_3L(H_2O)\cdot 0.5H_2O\cdot NCMe$	$Nd_2(NO_3)_6L_2$	$[GdL(NO_3)_2(H_2O)_3]\cdot(NO_3)\cdot 3H_2O$	$[Er(NO_3)_2L](NO_3)$	$[Y(NO_3)_2L(H_2O)](NO_3)$	$Y_2(NO_3)_6L_2$
Empirical formula	C30H30La2N16O20	C30H30Ce2N16O20	C17H19N9O10.5Pr	C30H26N16O18Nd2	C15H25GdN8O15	C15H13ErN8O12	C15H15N8O11Y	C30H26N16O18Y2
Formula weight	1212.52	1214.92	658.32	1187.14	714.68	664.60	570.26	1076.48
Crystal system, space group	Triclinic, $P\bar{1}$	Triclinic, $P\bar{1}$	Triclinic, $P\bar{1}$	Monoclinic, $P2_1/c$	Triclinic, $P\bar{1}$	Triclinic, $P\bar{1}$	Triclinic, $P\bar{1}$	Monoclinic, $P2_1/c$
a/Å	8.126(14)	8.135(14)	9.248(16)	10.932(17)	8.183(14)	7.652(13)	9.212(11)	10.886(16)
b/Å	9.638(17)	9.611(17)	12.976(18)	14.53(2)	9.585(14)	10.803(17)	10.887(14)	14.401(18)
c/Å	14.08(2)	14.05(2)	12.967(15)	13.23(2)	16.57(2)	14.55(2)	12.361(14)	13.191(18)
α/°	92.13(1).	92.30(1)	60.46(1)	(90)	82.41(1)	95.91(1).	104.70(1)	(90)
β/°	101.89(1)	101.36(1)	86.00(1)	107.91(1)	82.38(1)	101.43(1)	98.63(1)	108.51(1)
γ/°	100.31(1).	100.43(1)	89.33(1)	(90)	78.88(1)	95.43(1)	107.55(1)	(90)
V/Å3	1059	1056	1350	2000	1257	1165	1108	1961
Z, calculated density/Mg m^{-3}	1, 1.902	1, 1.911	2, 1.619	2, 1.972	2, 1.889	2, 1.895	2, 1.715	2, 1.823
μ/mm^{-1}	2.090	2.229	1.870	2.666	3877	3598	3745	6642/3811
Reflections collected/unique	3527	3492	4745	6657/3811	3877/0/354	3598/0/328	3745/0/326	3811/0/301
Data/restraints/parameters	3527/0/309	3492/0/309	4745/0/355	3811/0/301				
Final R indices[$I>2\sigma(I)$]$R1$, $wR2$	0.0297, 0.0777	0.0942, 0.2189	0.1015, 0.2625	0.0234, 0.0614	0.0482, 0.1278	0.0568, 0.1657	0.0766, 0.1981	0.0807, 0.2013
R indices (all data)	0.0350, 0.0806	0.1606, 0.2524	0.1173, 0.2727	0.0294, 0.0650	0.0559, 0.1345	0.0694, 0.1793	0.1118, 0.2226	0.1259, 0.2307
Largest diff. peak and hole/e Å^{-3}	0.816, −0.954	1.705, −1.161	2.600, −1.413	0.0850, −0.652	1.632, −1.780	1.502, −1.561	0.948, −1.569	1.861, −1.513

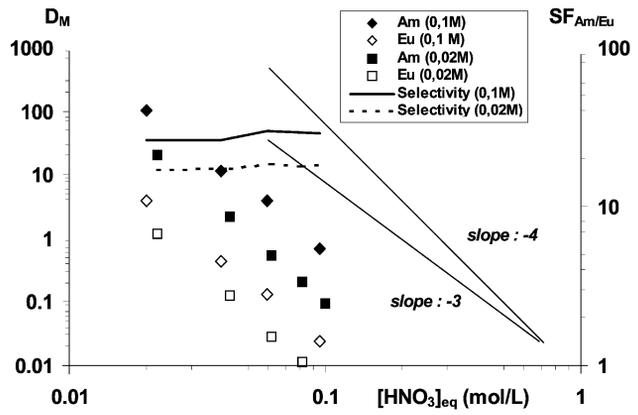

Fig. 3 The distribution coefficients (D_M) and separation factors ($SF_{Am/Eu}$) as a function of the nitric acid concentration for *ethyl,hemi-BTP*.

R,hemi-BTP at higher acidities. In principle, with the BTP reagents the extraction of Am(III) is not dependent on the concentration of the synergist, eqn. (2).

$$Am(III) + 3[NO_3]^- + 3BTP = [Am(III)(BTP)_3]^{3+}[NO_3]^-_3 \quad (2)$$

Thus, it is clear that the mechanism for the extraction of minor actinides by the *hemi-BTPs* resembles that of terpyridine rather than that of the BTPs.

Nuclear magnetic resonance studies.

Yttrium(III) nitrate and *Me,hemi-BTP*. The ^{1}H NMR titration curve for *Me,hemi-BTP* against yttrium(III) nitrate in acetonitrile is shown in Fig. 4. Since the rate of exchange was sufficiently slow to allow the observation of different ^{1}H NMR peaks for each species containing *Me,hemi-BTP*, the relative concentrations of these species were measured using a method similar to that used to investigate the coordination chemistry of beryllium.[33] Two metal-containing species may be identified with metal : *Me,hemi-BTP* ratios of 1 : 1 and 1 : 2. The first equilibrium constants between the yttrium nitrate and the *Me,hemi-BTP* is very high. The second constant was estimated to be 650(220) mol^{-1} dm^3. These species are similar to those observed for terpyridines but there was no evidence for a 1 : 3 complex.

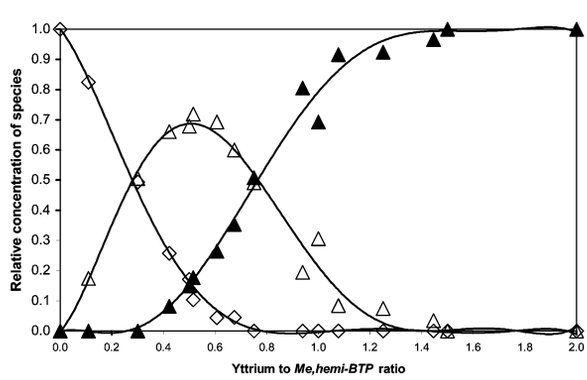

Fig. 4 NMR titration curve of *Me,hemi-BTP* against yttrium(III) nitrate. Key: free ligand (L) ◇, [YL] ▲, and [YL$_2$] △.

Lanthanum(III) nitrate and *Me,hemi-BTP*. For lanthanum(III)–*Me,hemi-BTP* complexes, the rate of ligand exchange was so high that only one peak was observed for each proton (see Fig. 5). Therefore, a similar method to that established for rapidly exchanging thallium crown ether complexes was used.[34,35]

A single break in the graph of $\Delta\delta$ *vs.* [La]/*Me,hemi-BTP* was seen for each peak. For one peak (Hc) the intercept was at 0.98

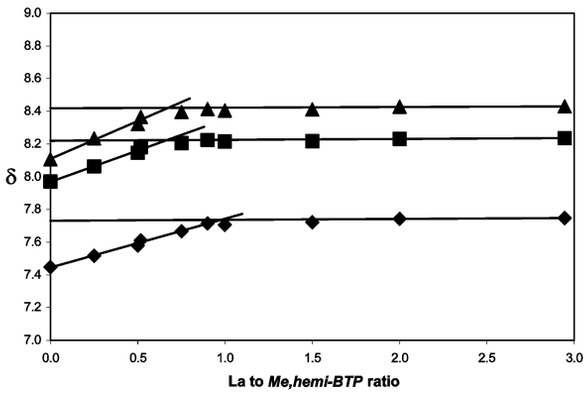

Fig. 5 NMR titration – the variation of chemical shift (δ) observed for three separate peaks on addition of lanthanum nitrate to *Me,hemi-BTP* in acetonitrile. Key: Ha ◆, Hb ■, and Hc ▲, see Fig. 6.

equivalents of lanthanum. Therefore, a complex with a metal : *Me,hemi-BTP* ratio of 1 : 1 was formed. The intercepts for the two other peaks (Ha and Hb) were at 0.67 and 0.66 (respectively) imply that there may also have been a 1 : 2 complex. There was no evidence for a 1 : 3 complex even though the very high permittivity of acetonitrile (ε = 37.5) favours the separation of the anionic nitrate ligands from the cationic metal centres. The significantly lower relative permittivities of dodecane and tributyl phosphate, which are 2 and 8, respectively, favour the binding of nitrate to the metals and so the formation of the 1 : 3 complex is disfavoured.

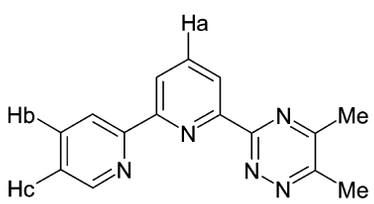

Fig. 6 Structure of *Me,hemi-BTP* showing the selected proton environments.

Resistance of the reagents to decomposition

It is known that the BTP ligands are decomposed by contact with nitric/nitrous acid mixtures, and it was of interest to establish whether the *hemi-BTP* reagents would resist this acid-induced decomposition. In the absence of nitrous acid, it was found that *Et,hemi-BTP* could be quantitatively recovered from 3 M nitric acid. However, when nitrous acid was present together with nitric acid, the compound *Et,hemi-BTP* was decomposed giving 2,2′-biipyridyl-6-carboxylic acid as one of the products. It is clear that there was destruction of the 1,2,4-triazine ring, and only the 2,2′-bipyridine portion of compound *Et,hemi-BTP* remained intact. Thus it appears that both the *hemi-BTPs* and the BTPs are unstable in the presence of nitrous acid. Nitrogen monoxide, for example, may be present as a decomposition or reduction product of nitrous acid.[36] The free radical reaction of nitrogen oxides with alkylarenes at the benzylic site is one possible mechanism for the degradation of the ligand by the mixture of nitric acid and sodium nitrite.

Crystallography

X-Ray crystallography was used to establish the detailed structures of the complexes. These detailed structures are consistent with the NMR results measured on the organic phase. The crystalline solids obtained by the reaction of *Me,hemi-BTP,* **3** in Fig. 1, in acetonitrile with either a lanthanide or Group III nitrate were found to be either 1 : 1 mono- or 2 : 2 di-nuclear coordination complexes. Water was found within the inner coordination sphere of all the mononuclear complexes, while

Table 5 Dimensions (Å) in the metal coordination spheres for the complexes

(a) The dimers

	La	Ce	Nd	Y
M–N(11)	2.676(5)	2.697(11)	2.573(5)	2.484(7)
M–N(21)	2.685(6)	2.664(12)	2.603(4)	2.520(6)
M–N(31)	2.672(5)	2.657(12)	2.597(4)	2.519(6)
M–O(41)	2.607(5)	2.566(11)	2.544(4)	2.484(6)
M–O(42)	2.694(6)	2.682(12)	2.534(4)	2.445(6)
M–O(51)	2.597(5)	2.540(12)	2.517(4)	2.434(6)
M–O(52)	2.863(6)	2.959(17)	2.519(5)	2.427(6)
M–O(61)$1	2.627(5)	2.585(12)	2.583(4)	2.491(6)
M–O(62)$1	2.685(4)	2.672(10)	2.624(4)	2.588(5)
M–O(62)	2.599(4)	2.595(10)	2.527(4)	2.414(5)
M–O(100)	2.564(5)	2.528(12)	–	–

(b) The monomers

	Pr	Gd	Er	Y
M–N(11)	2.582(12)	2.553(7)	2.478(10)	2.493(7)
M–N(21)	2.586(11)	2.563(7)	2.504(8)	2.493(7)
M–N(31)	2.535(13)	2.592(7)	2.469(8)	2.495(7)
M–O(41)	2.501(12)	–	–	–
M–O(42)	2.558(12)	–	–	–
M–O(51)	2.512(12)	2.459(6)	2.423(8)	2.453(6)
M–O(52)	2.520(11)	–	2.428(9)	2.433(6)
M–O(61)	2.538(13)	2.457(6)	2.391(8)	2.404(6)
M–O(62)	2.493(11)	2.628(7)	2.455(9)	2.447(6)
M–O(100)	2.394(10)	2.355(5)	2.331(7)	2.323(6)
M–O(200)	–	2.401(6)	2.300(8)	2.296(6)
M–O(300)	–	2.427(6)	–	–

examples of dinuclear complexes with and without water ligands were observed. While the stoichiometry of the lanthanide complexes of both **1** and **2** varies within the range of 1 : 1 to 1 : 3,[37] all the complexes of *Me,hemi-BTP* observed by crystallography possessed an organic ligand to metal ratio of 1 : 1. Apart from yttrium(III) the reactions of *Me,hemi-BTP* with the metal nitrates furnished only one crystalline solid. Yttrium(III) formed 1 : 1 mono- or 2 : 2 di-nuclear coordination compounds. It is noteworthy that we found no examples of $[LaL_3]^{3+}$ which is so prevalent for L = BTP with the *hemi-BTPs*. The dimensions in the metal coordination sphere of the complexes are given in Table 5.

Two of the structures are isomorphous, namely those with M = La and Ce(III). The structure of this $La_2L_2(NO_3)_6(H_2O)_2$ dimer (L = *Me,hemi-BTP*) is shown in Fig. 7 together with part of the atomic numbering scheme – there are more in Fig. 9. The dimers contain a crystallographic centre of symmetry. Each metal is eleven-coordinate being bonded to three nitrogen atoms of the terdentate ligand, two bidentate nitrate anions and a water molecule. In addition, each metal is bonded to two bridging nitrates, which are bidentate to one lanthanide and monodentate to the other. The dimensions of the three Ln–N bonds are equivalent in the two structures within experimental error. However, there are significant differences in the bonding patterns of the two bidentate nitrate anions since in both cases one bond is significantly longer than the other. For O(41) and O(42) in the non-bridging nitrate, the distances differ by 0.087, 0.116 Å for La, Ce but there is an even larger difference between bond lengths to O(51) and O(52) being 0.266, 0.419 Å for La and Ce(III), respectively. Clearly, the latter nitrate is bordering on being monodentate rather than bidentate. The distances of the bonds from the metals to the bridging nitrate ligand are more similar. The bond to water is the shortest of the bonds in both cases at 2.564(5), 2.528(12) Å for M = La or Ce, respectively. There are two equivalent weak hydrogen bonds in the dimer between O(100) and N(36) with O ··· N distances of 3.32 Å and Ln–O(100) ··· N(36) angles of 118.6° with M = La and 3.29 Å, 118.2° for M = Ce. There is also a weak hydrogen bond between C(12)–H and O(61) (see Fig. 9) with H ··· O

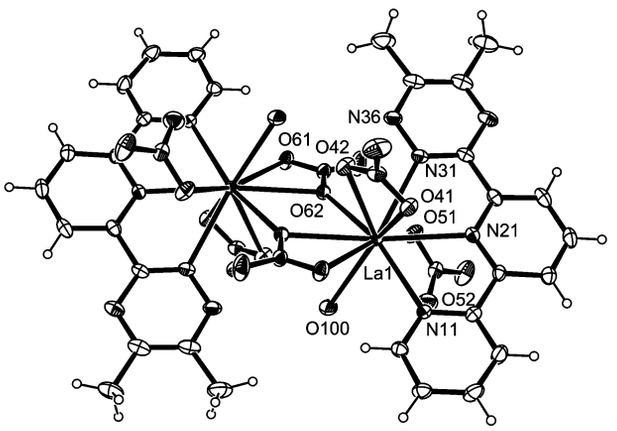

Fig. 7 The centrosymmetric structure of the dimer $La_2L_2(NO_3)_6$-$(H_2O)_2$ with ellipsoids at 30% occupancy; L = *Me,hemi-BTP*. The structure of the Ce-dimer is isostructural. The hydrogen atoms on the water molecules were not located.

distances of 2.41, 2.40 Å and C–H ⋯ O angles of 122, 122° with M = La, Ce, respectively. The cerium(III) complexes of polydentate aromatic nitrogen heterocyclic ligands include compounds with metal to organic ligand ratios of 1 : 1,[38] 1 : 2[39] and 1 : 3. Terpyridine, ligand **1**, forms mononuclear 1 : 1 complexes with cerium(III), while butylaminoditertiarypyridinetriazine forms a mononuclear 1 : 1 complex with cerium(IV) nitrate.[40]

The Nd complex shown in Fig. 8 is also a dimer, but of stoichiometry $Nd_2L_2(NO_3)_6$ (L = *Me,hemi-BTP*), and is equivalent to that found for the La and Ce complexes but without the additional bonded water molecules. The metal atoms are ten-coordinate, and the bond lengths in the metal coordination sphere are much more regular than is the case with the La and Ce complexes. Thus all the Nd–N distances are similar ranging from 2.573(5) to 2.603(4) Å. The M–O distances for the bidentate nitrates range from 2.517(4) to 2.544(4) Å. There is a slight elongation in the bond to the bridging nitrate, but the longest distance is only 2.624(4) Å. There are two equivalent weak hydrogen bonds in the dimer between C(12)–H and O(51) with an H ⋯ O distance of 2.60 Å and a C–H ⋯ O angle of 131°, and as discussed later these could play a significant role in the mechanism of partitioning. Prior to this study, dimers had only been observed previously for the BTP ligands, and no other terdentate nitrogen ligands. The structures of $[Pr_2L^1{}_2(NO_3)_6]$ and $[Nd_2L^1{}_2(NO_3)_6]$, L^1 = propyl-BTP reported recently[37] have centrosymmetric structures equivalent to that of the $Nd_2L_2(NO_3)_6$ (L = *Me,hemi-BTP*) complex reported here. The structures with two nitrates bridging two lanthanides are also relatively rare. A search of the Cambridge Crystallographic Database[41,42] revealed only six complexes with Ln–O(nitrate)–Ln bridges, of which three are isomorphous. In addition, there are eight further dimeric structures containing Ln–O–N–O–Ln bridges of which three are isomorphous. The O–Nd–O angle in the Nd_2O_2 ring is 58.26°. The literature range for this angle in Ln_2O_2 rings containing bridging nitrate oxygen atoms, is 55 to 65°, and all such rings are planar.

There are few differences between the bonding of the pyridine and 1,2,4-triazine rings to the metal, but there are small differences in the case of the praesodymium complex. The structure of $[Pr(NO_3)_3(H_2O)$*Me,hemi-BTP*$]$ is shown in Fig. 9. The metal atom is ten-coordinate being bonded to three nitrogen atoms of the terdentate ligand, three bidentate nitrate anions and a water molecule. Of the three bonds from the metal to the terdentate nitrogen ligand, the Pr–N(31) bond at 2.535(13) Å is significantly shorter than the Pr–N(11) bond at 2.582(12) Å. This decrease in the bond length may arise from the stronger electrostatic attraction between Pr and N(31) compared with Pr–N(11) and Pr–N(21) of the dipyridine part of the molecule. The three nitrates are relatively symmetrically bonded with differences of up to 0.060 Å between the M–O bond lengths. The Pr–O(100) bond is the shortest of all at 2.394(10) Å. There is likely to be an intramolecular hydrogen bond from O(100) to the triazine nitrogen atom N(36) at 2.87 Å. In addition C(12)–H forms two weak hydrogen bonds to O(52) and O(62) with H ⋯ O distances at 2.79 and 2.64 Å.

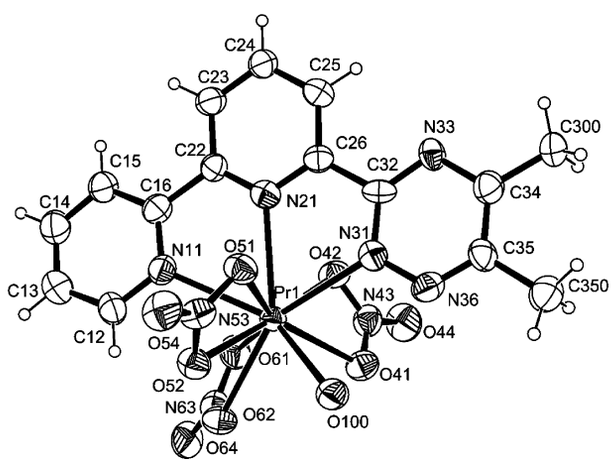

Fig. 9 The structure of $Pr(NO_3)_3(H_2O)$*Me,hemi-BTP* with ellipsoids at 30% probability. The hydrogen atoms of the water molecule were not located.

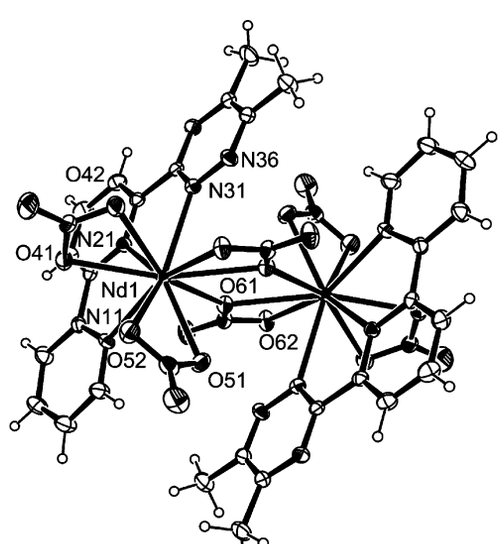

Fig. 8 The structure of the $Nd_2L_2(NO_3)_6$ (L = *Me,hemi-BTP*) dimer with ellipsoids at 30% probability. The hydrogen atoms of the water molecule were not located.

All the metal centres and nitrates, and the vast majority of the waters are arranged into one-dimensional channels, which are all arranged in a parallel manner. The remainder of the solid consists of the aromatic rings of *Me,hemi-BTP*. Similar ordering can be seen in a manganese phenanthroline benzene-1,3,5-tricarboxylate.[43]

The smaller lanthanide elements Gd and Er both form monomers with *Me,hemi-BTP*. The structure of the $[Gd(NO_3)_2$-$(H_2O)_3$*Me,hemi-BTP*$]^+$ cation is shown in Fig. 10. The metal cation is nine-coordinate being bonded to three nitrogen atoms of the terdentate nitrogen ligand *Me,hemi-BTP*, three oxygen atoms from two nitrates, one bidentate and one monodentate, and three water molecules. For the monodentate nitrate the two distances are Gd(1)–O(51) 2.459(6) and Gd(1)–O(52) 3.144(8) Å indicating that there is little interaction between the second oxygen and the metal. In this case the three bonds (M–O(100); M–O(200); M–O(300)) from the metal to water are mutually *cis* with angles of 77.3(2), 83.9(2) and 69.5(2)°. There are hydrogen bonds between N(36) and O(100) (O ⋯ N at 3.08 Å) and also

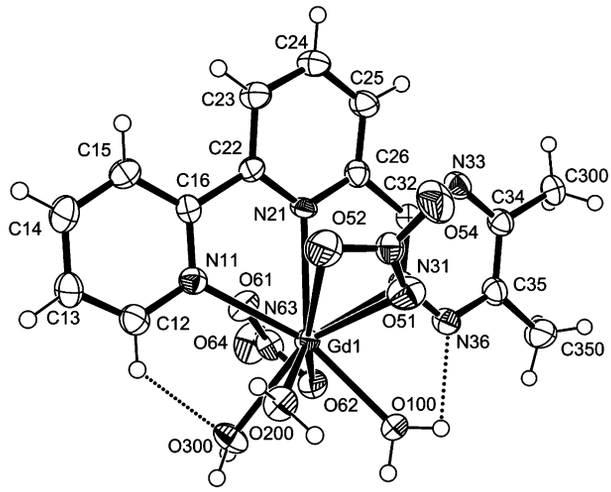

Fig. 10 The structure of $[Gd(NO_3)_2(H_2O)_3$*Me,hemi-BTP*$]^+$ with ellipsoids at 30% probability. The hydrogen bonds between C(12)–H and O(300) as well as between O(100) and N(36) stabilise this complex. Similarly, intramolecular hydrogen bonding stabilises other complexes with *R,hemi-BTPs*.

from N(36) to a solvent water molecule O(500) (O ··· N 3.08Å) and also between C(12)–H and O(300) (H ··· O 2.62 Å), which stabilise the coordination sphere – as discussed later. The other nitrate can be considered as bidentate although the two bond lengths differ significantly at 2.457(6) for Gd(1)–O(61) and 2.628(7) Å for Gd(1)–O(62). In common with *Me,hemi-BTP*, the reaction of terpyridine (**1**) with gadolinium nitrate forms a solid containing the complex mononuclear cation $[Gd(NO_3)_2(H_2O)_3($**1**$)]$ together with nitrate counter ions.[44]

Within the crystal structure, the hydrophobic portion of *Me,hemi-BTP* is arranged in layers separated by layers of nitrates, waters and metal atoms (see Fig. 11). Similar layering has been observed in the structures of lead(II) carboxylates[45] and in a hydrated copper(II) alkylsulfonate.[46]

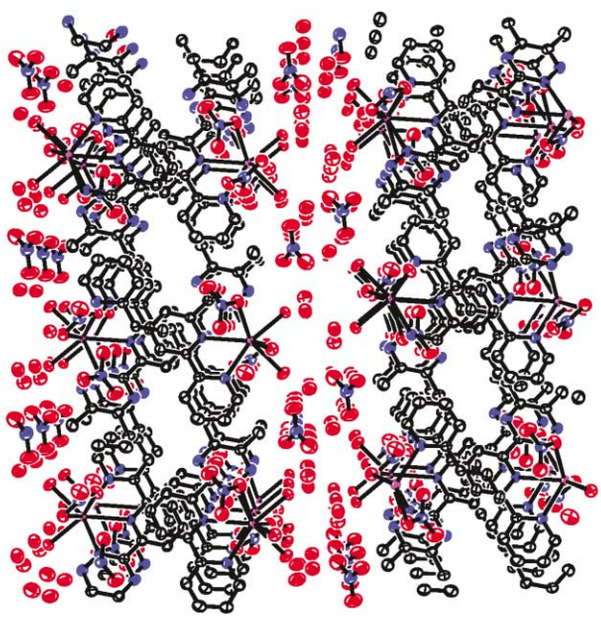

Fig. 11 Crystal structure of $[Gd(NO_3)_3(H_2O)_3$*Me,hemi-BTP*$]$ showing layers of water and nitrates. (For clarity all hydrogens are excluded.)

The structure of the erbium complex shows discrete $[Er(NO_3)_2(H_2O)_2$*Me,hemi-BTP*$]^+$ cations and nitrate anions, Fig. 12. The metal is therefore nine-coordinate being bonded to three nitrogen atoms of the terdentate ligand, two bidentate nitrates and two water molecules. The two water molecules are mutually *cis* with a O(100)–Er(1)–O(200) angle of 86.3(3)°. It is

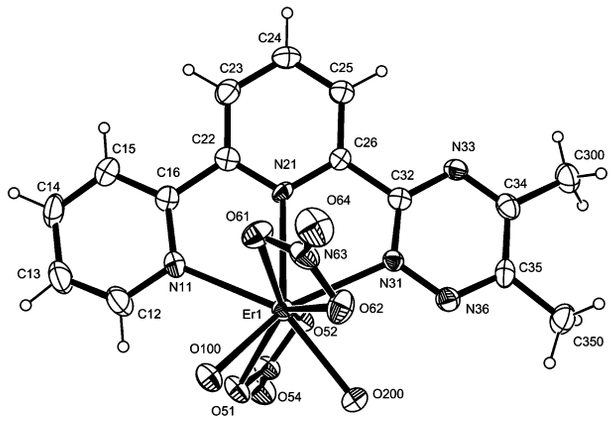

Fig. 12 Structure of the $[Er(NO_3)_2(H_2O)_2$*Me,hemi-BTP*$]^+$ cation. The hydrogen atoms of the water molecule were not located.

possible that complexes with these alternate structures co-exist in solution. The molecular dimensions show some unusual features. Unlike the monomeric Pr structure, the two bonds Er–N(11) and Er–N(31) are equivalent but are shorter than the central Er–N(21) bond. Of the two nitrates, one is symmetrically bonded while the other shows long (M–O(62) 2.455(9) Å) and short (M–O(61) 2.391(8) Å) bonds. As is usually the case, the bonds from the lanthanide metal to the water molecules are the shortest of the bonds at 2.300(8), 2.331(7) Å. The molecule contains two intramolecular hydrogen bonds between the water molecules and the bonded nitrates, which is a common feature of these types of structures. Thus C(12)–H(12) ··· O(100) (C ··· O 3.15, H ··· O 2.70 Å) is a hydrogen bond from an aromatic hydrogen to a water molecule and O(200)–N(36) 2.78 Å represents a hydrogen bond from a hydrogen on a water molecule to a triazine nitrogen atom.

This erbium compound is not structurally similar to that formed with terpyridine (**1**), which forms mononuclear neutral complexes $[Er(NO_3)_3($EtOH$)($**1**$)]$ and $[Er(NO_3)_3(H_2O)($**1**$)]\cdot$**1**.[47] The second terpyridine in the latter complex is hydrogen bonded to the metal-bound water.

The reaction of yttrium nitrate and *Me,hemi-BTP* gave a mixture of two different crystalline mononuclear complexes. One of these contains a hydrated nine-coordinate cationic complex, which has the same stoichiometry as that found for Er – $[Y(NO_3)_2(H_2O)_2$*Me,hemi-BTP*$]^+$ together with a nitrate anion, Fig. 13. However, the geometry of the coordination sphere is rather different in that C(12)–H is hydrogen bonded to a nitrate oxygen atom O(51) rather than a water molecule, the H ··· O distance being 2.51 Å. However, there is still a hydrogen bond interaction between a water molecule O(200) and N(36), in this structure the O ··· N distance is 2.67 Å. The two

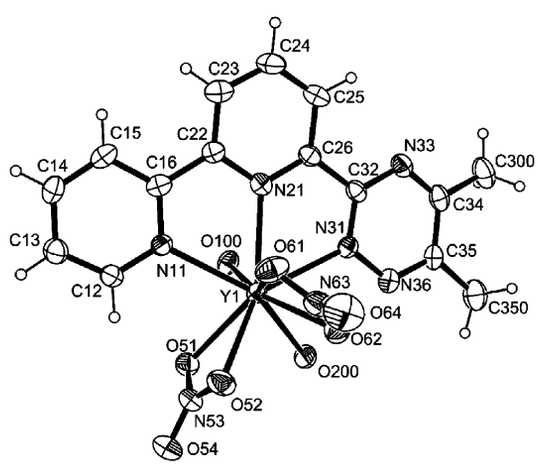

Fig. 13 The crystal structure of $[Y(NO_3)_2(H_2O)_2$*Me,hemi-BTP*$]^+NO_3^-$. The hydrogen atoms of the water molecule were not located.

Table 6 Some crystallographic data of the compounds

Metal	Nuclearity: monomer or dimer	Coordination number	Metal–nitrogen bond length/Å			{M–N(31) − M–N(11)}/Å
			Triazine N(31)	Inner pyridine N(21)	Outer pyridine N(11)	
Y	M	9	2.495(7)	2.493(7)	2.493(7)	0.002
Y	D	10	2.519(6)	2.520(6)	2.484(7)	0.035
La	D	11	2.672(5)	2.685(6)	2.676(5)	−0.006
Ce	D	10	2.657(12)	2.664(12)	2.697(11)	−0.040
Pr	M	10	2.535(13)	2.586(12)	2.582(12)	−0.047
Nd	D	10	2.597(4)	2.603(4)	2.573(5)	0.024
Gd	M	9	2.592(8)	2.563(7)	2.553(7)	0.039
Er	M	9	2.469(8)	2.503(8)	2.478(10)	−0.009
						mean −0.002

water molecules form the shortest bonds to the metal, O(100) at 2.323(6) and O(200) at 2.296(6) Å. The two nitrate groups are bidentate with Y–O distances ranging between 2.404(6) and 2.447(6) Å. The three Y–N(11), –N(21) and –N(31) distances are equivalent at 2.493(7), 2.493(7), 2.495(7) Å – suggesting that there is no difference in metal-binding with the pyridine and triazine rings. There is a clear parallel with terpyridine, with which it is possible to form $[Y(NO_3)_2(H_2O)_2(\mathbf{1})]\cdot NO_3\cdot 2H_2O$ by a similar reaction.[29] and neutral mononuclear complexes $[Y(NO_3)_3(H_2O)(\mathbf{1})]$ and $[Y(NO_3)_3(H_2O)(\mathbf{1})]\cdot\mathbf{1}\cdot 3MeCN$.[48]

The second yttrium structure is, however, a centrosymmetric dimer similar to that observed for the Nd dimer complex, Fig. 8, in which the metal atoms are nine-coordinate. Despite the difference in size between neodymium and yttrium, the two structures are remarkably similar although, as expected, the bond lengths are about 0.15 Å shorter in the latter dimeric complex. Again dimer formation is facilitated by two equivalent hydrogen bonds between C(12)–H and O(51) with H ⋯ O 2.51 Å.

Comparison of the Ln–N bond lengths in the metal complexes. It was thought that the triazine ring nitrogen N(31) might bind more strongly to the metal atom than do the inner N(21) and outer N(11) pyridine nitrogens. From Table 6, which details the M–N bond lengths, it is clear that there is no general tendency for the metal triazine nitrogen bond length to be shortened. All metal–nitrogen distances are within the literature range for lanthanide complexes of both terpyridine and BTPs. Since the same core of two metal atoms and six nitrates is present in the neodymium complexes of tetramethyl-BTP and tetrapropyl-BTP, it is possible to make a direct comparison between these two complexes. It was found that the bond lengths in the complexes of *Me,hemi-BTP* were not significantly different to those of the BTPs. In previous studies, the geometries of the $[Ln(terpy)_3]^{3+}$ and $[Ln(BTP)_3]^{3+}$ cations were compared for La(III), Ce(III) and U(III), and it was found that for any given metal, the M–N(BTP) distances are shorter than the M–N(terpy) distances by values up to 0.05 Å for La and Ce but by nearly double this figure (0.09 Å) for U. This was ascribed to the better affinity and selectivity of the BTPs by comparison with terpy in the complexation of trivalent 4f and 5f ions. However, our results are not consistent with this observation because the Ln–N bond lengths in the *R,hemi-BTP* complexes show that in some structures the bond to the triazine nitrogen atom N(31) is indeed shorter than that to the pyridine nitrogen atom N(11), but in other cases the reverse is found to be the case. Of course, in the present series of structures, an exact comparison is difficult to make because the environments of N(11) and N(31) in the coordination sphere are often different. A small potential difference in bond strength between M–N(31) and M–N(11) could well be negated by steric effects, which together with hydrogen bond formation or even packing effects could result in a reversal of differences in bond lengths. Indeed, the frequent variation in M–O distances in these compounds support this view. From data on terpy structures in the Cambridge Crystallographic Database, it is clear that there is a significant variation in bond length depending on the nature of the complex formed. Thus there are nine examples of La(terpy) structures with mean bond lengths of 2.682(25), 2.694(23) Å for outer and inner ring nitrogens, respectively, and five examples of Er(terpy) structures with mean distances of 2.488(17), 2.500(22) Å, respectively, the high standard deviations indicating the large spread of values. We conclude that any change in bond length between pyridine nitrogen and triazine nitrogen is too small to observe in the context of variations in Ln–N distance owing to the environment of the coordination sphere.

The possible role of hydrogen bonds in structure and in partitioning. An additional point of interest in the structures reported here with the complexes containing *R,hemi-BTPs* is the fact that water molecules are more commonly found in the metal coordination sphere than is the case for other terdentate ligands. This may be due to the stabilising factor of hydrogen bond formation, which is a common part of coordination spheres of lanthanides with terdentate ligands.[18] Indeed, the arrangement of the ligands in the coordination sphere facilitates the formation of these hydrogen bonds in these *R,hemi-BTP* complexes as was also found with terpy complexes.[18] With ligands such as terpyridine, there are usually two donor hydrogen bonds formed from the *ortho*-hydrogen atoms on the outer pyridine rings to nitrates or water molecules in the coordination sphere. However, with the present *R,hemi-BTP* ligand, there is no such C–H group on the triazine ring but rather a nitrogen atom, which can only form hydrogen bonds with the hydrogen atom from water molecules, but in the absence of a hydrogen atom cannot form any type of hydrogen bonds with nitrate anions.

As is shown in six of the structures reported here, there is a water molecule in the coordination sphere, which forms such a hydrogen bond with N(36). The exceptions are the Nd and Y dimers, which do not contain water molecules. In all eight structures, however, the –C(12)–H moiety does form hydrogen bonds. This feature of these structures with *R,hemi-BTPs* may indicate a reason for the different extraction properties of the terpy, *R,hemi-BTP* and BTP ligands. It has been remarked previously that a unique feature of the chemistry of the BTP ligand is the facile formation of the $[M(BTP)_3]^{3+}$ cation with the exclusion of nitrates from the coordination sphere. It has been previously postulated that this is due to the electronic differences of the two ligands.[49] However, it is reasonable to consider the possibility that nitrates are not found in the coordination sphere of the BTPs because they cannot be stabilised by hydrogen bond formation. This is not the case with terpy or indeed with the *R,hemi-BTPs*. It is clearly possible that the ease of formation of

hydrogen bonds has a significant effect on distribution coefficients and separation factors. It has been demonstrated that intramolecular hydrogen bonding plays a critical role in the formation of the coordination sphere of the metal cation. The hydrogen bonding also explains why ligands such as the BTPs, which do not form the intramolecular hydrogen bonds, are able to form $[ML_3]^{3+}$ cations that are efficient in partitioning.

Computational chemistry

Conformations adopted by the free *R,hemi-BTPs*. The electronic properties of the free *R,hemi-BTPs* have been compared to those of terpyridine and to the BTPs. The charges on the nitrogen atoms in the three ligands at the HF/6-31+G* level of theory have been calculated using the Gaussian98 program.[50] There are four possible conformations for the *R,hemi-BTP* which can be described as *cc*, *ct*, *tt*, *tc*, the first letter describing the torsion angle N(11)–C–C–N(21) between the outer pyridine ring and the central pyridine ring and the second letter that between the triazine ring and the central pyridine ring N(21)–C–C–N(31) (see Fig. 14). Energies at the HF/631+G* level after geometry optimisation were −769.74732, −769.74982, −769.76049 and −769.75924 a.u.. The lowest energy conformation is the *tt* but the *tc* is only 0.78 kcal mol^{-1} higher in energy. This small difference relates to the fact that there are no *ortho*-hydrogen atoms in the triazine ring to increase the steric energy. By contrast the *ct* conformation is 9.0 kcal mol^{-1} higher in energy because of unfavourable interaction between two adjacent *ortho*-hydrogen atoms (illustrated in Fig. 14), which cause the rings to twist away from coplanarity. The *cc* conformation has the highest energy, which is the conformation found in the metal complexes but clearly not in the free ligand. It is likely that the lowest energy *tt* conformation is to be found in solution and therefore metal complexation needs to be accompanied by a change in ligand conformation. The energy barriers were calculated *via* a scan calculation at the HF/6-31+G* level using a torsion angle rotation in 22.5° intervals in the absence of metal for the conformational change of *tt* to *tc*, and *tt* to *ct* and obtained values of 4.09, 6.92 kcal mol^{-1}, respectively, thus confirming the relative ease of rotation for the triazine ring compared to the pyridine ring.

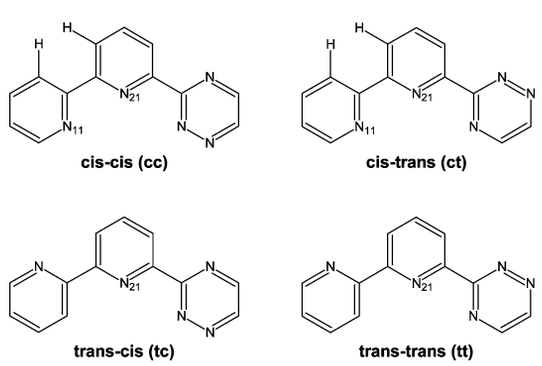

Fig. 14 Nitrogen atoms, which can be protonated to form low energy conformations in *R,hemi-BTPs* are named.

All low energy conformations are stabilised by the formation of intramolecular hydrogen bonds. Those *ortho*-hydrogens on carbon atoms which are involved in steric repulsions that cause ring-rotation are illustrated in the conformations where this repulsion occurs. In some protonated structures a similar interaction occurs between N–H and C–H *ortho*-hydrogens.

Charge distribution. For the *R,hemi-BTPs* the charges on the five independent nitrogen atoms were found to be N(11) −0.52; N(21) −0.56; N(31), −0.31; N(33) −0.55 and N(36) −0.22. These results can be compared to those obtained for the symmetrical terpyridine (N(11), N(31) −0.52 and N(21) −0.56) and BTP ligands (N(21) −0.56; N(11), N(31) −0.31; N(13), N(33); −0.55 and N(16), N(36) −0.22). Clearly, the striking result here is the large difference in charge between the donor nitrogen atom from a pyridine ring (outer −0.52, inner −0.56) and that of a 1,2,4-triazine ring (−0.31). Indeed in the triazine ring the sum of the charges on the two adjacent nitrogens is equivalent to that of the one nitrogen in terpyridine. This large change in charge distribution may well be a contributing factor to the unique selection properties of the BTP ligand. It is interesting to note that the charge distribution for atoms in the outer pyridine and triazine rings in the *R,hemi-BTP* ligand is similar to those found in the symmetrical terpy and BTP ligands, confirming that the electronic properties of *R,hemi-BTP* are intermediate between those of terpyridine and the BTP ligands, and that the two outer rings are to some extent independent of each other. The total ring charges also reflect this property being 0.008, 0.033, −0.042 for rings 1,2,3 in the *hemi-BTP*, 0.002*2, and −0.004 in terpy, and −0.036*2, 0.071 for rings 1,3 and 2 in BTP.

Table 7 Relative energies (kcal mol^{-1}) of protonated *hemi-BTP* conformers. Low energy conformations are shown in bold

	Conformer			
Protonated nitrogen	*cc*	*ct*	*tc*	*tt*
N(11)	**2.87**	**3.90**	11.47	11.65
N(21)	**0.00**	**0.82**	**4.69**	**6.35**
N(31)	31.84	33.15	26.80	27.77
N(36)	11.74	25.85	9.57	20.43
N(33)	40.75	22.98	34.97	22.18

Protonation. The extraction process is carried out in nitric acid and, therefore, it was of interest to investigate the protonation pattern to be found in the *R,hemi-BTPs*. There are four different conformations of the ligand and five different nitrogen atoms that potentially could be protonated so twenty geometry optimisations were carried out at the HF/6-31+G* level with the results shown in Table 7.

For each conformer it is noticeable that the lowest energy protonation site is always on the central pyridine atom N(21), although in the *cc* or *ct* conformations the energy for protonation on the pyridine N(11) is similar. When N(21) is protonated in the *cc* or *ct* conformation, then the structure is stabilised by hydrogen bond interactions between the N–H group and the nitrogen atoms on the two adjacent rings. When N(11) is protonated in these conformations there can be only one such interaction. When N(21) is protonated in the *tc* or *tt* conformations, there is also only one adjacent nitrogen atom available for hydrogen bonding, but now there are interactions between adjacent *ortho*-hydrogen atoms (see Fig. 14) that give rise to steric repulsions between adjacent rings and cause rotations that reduce conjugation. All other structures of the protonated *R,hemi-BTP* have significantly higher relative energies and are unlikely to be formed.

It is interesting to note that the order of energies for the protonated species (viz *cc* < *ct* < *tc* < *tt*) is the exact opposite for that of the free ligand (*tt* < *tc* < *ct* < *cc*). It can therefore, be postulated that the protonation of the ligand facilitates the conformational change from *cc* to *tt* that is necessary for metal complexation. The metal then displaces the proton in the *tt* conformation to bind to the terdentate ligand. This could be a significant reason for the effectiveness of the terdentate nitrogen ligands in the extraction process in *acidic* nuclear waste.

Frontier orbitals. Calculations of the frontier orbitals were carried out for the *R,hemi-BTPs*, terpy and BTP in the lowest energy *tt* conformation (although the results from other conformations are similar) and are compared in Fig. 15. It is clear that there are strong similarities between the orbitals for the three ligands. All three HOMOs which are the π-donor orbitals

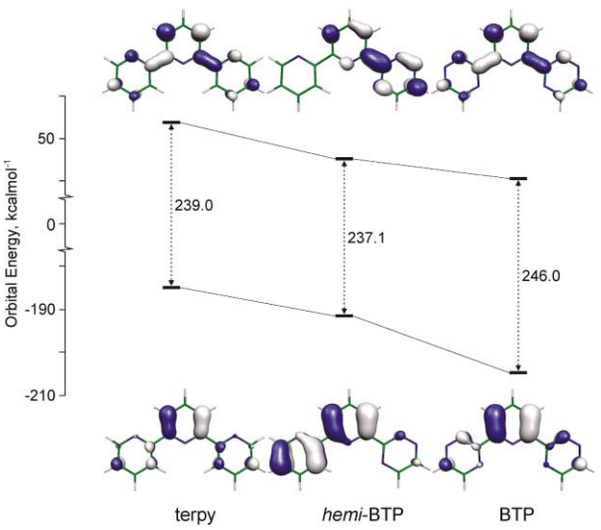

Fig. 15 A Walsh diagram showing the HOMO and LUMO orbitals and energies (kcal mol^{-1}) for terpy, *hemi-BTP* and BTP. Calculations were carried out using the *tt* conformation shown in Fig. 14.

contain a significant and equivalent contribution from the central pyridine ring. However, the contribution from the triazine rings is small in BTP and insignificant in the *R,hemi-BTPs*. By contrast the contribution from the outer pyridine ring is significant for both terpy but even more so in the outer pyridine ring of the *hemi-BTP*.

A slightly different pattern is observed for the LUMOs for which the contribution in both terpy and the BTPs is symmetric and involves all three rings. In the *R,hemi-BTPs* it is noticeable that the outer pyridine ring makes no contribution but the central nitrogen from the pyridine ring does make a contribution, which is not found in the other two symmetrical ligands. The contrast between the HOMO and LUMO for the *R,hemi-BTPs* is striking in that in the HOMO the triazine ring makes little contribution, while in the LUMO it is the pyridine ring that makes no contribution.

As is apparent from Fig. 15, the energies of the HOMOs and LUMOs of these ligands are consistent with the perception that the *hemi-BTP* is intermediate between terpy and BTP. Thus HOMO energies are terpy (−0.295 a.u.), *hemi-BTP* (−0.306 a.u.), BTP (−0.327 a.u) and LUMO energies are 0.065, 0.072, 0.085 a.u., respectively. In all three ligands there is a large difference in energy between the HOMO − 1 and HOMO orbitals, it being 0.037, 0.047, 0.051 a.u., respectively.

Conclusions

It has been established that 6-(5,6-dialkyl-1,2,4-triazin-3-yl)-2,2′-bipyridines (*R,hemi-BTPs*), have properties which are intermediate between those of the terpyridines and the bis(1,2,4-triazin-3-yl)pyridines (BTPs).

Acknowledgements

We are grateful for the financial support by the European Union Nuclear Fission Safety Programme (Contract FIKW-CT2000-0087). We would also like to thank the EPSRC and the University of Reading for funding of the image-plate system.

References

1 N. Boubals, M. G. B. Drew, C. Hill, M. J. Hudson, P. B. Iveson, C. Madic, M. L. Russell and T. Youngs, *J. Chem. Soc., Dalton Trans.*, 2002, 55–62.
2 G. R. Pabst, O. C. Pfueller and J. Sauer, *Tetrahedron*, 1999, **55**, 5047.
3 F. H. Case, *J. Org. Chem.*, 1966, **31**, 2398.
4 A. A. Schilt, T. A. Yang, J. F. Wu and D. M. Nitzki, *Talanta*, 1977, **24**, 685.
5 H. Chao, G. Yang, G.-Q. Xue, H. Li, H. Zang, I. D. Williams, L.-N. Ji, X.-M. Chen and X.-Y. Li, *J. Chem. Soc., Dalton Trans.*, 2001, 1326.
6 M. J. Hudson, M. R. S. Foreman, C. Hill, N. Huet and C. Madic, *Solvent Extr. Ion Exch.*, in the press.
7 M. Hägstrom, L. Spüth, A. Enarsson, J. O. Liljenzin, M. Skälberg, M. J. Hudson, P. B. Iveson, C. Madic, P. Y. Cordier, C. Hill and N. Francois, *Solvent Extr. Ion Exch.*, 1999, **17**, 221.
8 M. G. B. Drew, M. J. Hudson, P. B. Iveson, M. L. Russell, J.-O. Liljenzin, M. Skalberk, L. Spjüth and C. Madic, *J. Chem. Soc., Dalton Trans.*, 1998, 2973.
9 M. G. B. Drew, M. J. Hudson, P. B. Iveson, J.-O. Liljenzin, L. Spjüth, P.-Y. Cordier, A. Enarsson, C. Hill and C. Madic, *J. Chem. Soc., Dalton Trans.*, 2000, 821.
10 M. G. B. Drew, M. J. Hudson, P. B. Iveson, C. Madic and M. L. Russell, *J. Chem. Soc., Dalton Trans.*, 1999, 2433.
11 L. I. Semenova and A. H. White, *Aust. J. Chem.*, 1999, **52**, 507.
12 N. Boubals, M. G. B. Drew, C. Hill, M. J. Hudson, P. B. Iveson, C. Madic, M. L. Russell and T. G. A. Youngs, *J. Chem. Soc., Dalton Trans.*, 2002, 55.
13 M. G. B. Drew, M. J. Hudson, P. B. Iveson, C. Madic and M. L. Russell, *J. Chem. Soc., Dalton Trans.*, 2000, 2711.
14 M. Frechette and C. Bensimon, *Inorg. Chem.*, 1995, **34**, 3520.
15 L. I. Semenova and A. H. White, *Aust. J. Chem.*, 1999, **52**, 539.
16 C. J. Kepert, L. Wei-Min, L. I. Semenova, B. W. Skelton and A. H. White, *Aust. J. Chem.*, 1999, **52**, 481.
17 L. I. Semenova, A. N. Sobolev, B. W. Skelton and A. H. White, *Aust. J. Chem.*, 1999, **52**, 519.
18 M. J. Hudson, *Czech J. Phys.*, in the press.
19 Z. Kolarik, U. Mullich and F. Gassner, *Solvent Extr. Ion Exch.*, 1999, **17**, 23.
20 Z. Kolarik, U. Mullich and F. Gassner, *Solvent Extr. Ion Exch.*, 1999, **17**, 1155.
21 M. J. Hudson, M. G. B. Drew, D. Guillaneux, M. L. Russell, P. B. Iveson and C. Madic, *Inorg. Chem. Commun.*, 2001, **4**, 12.
22 J. C. Berthet, Y. Miquel, P. B. Iveson, M. Nierlich, P. Thuéry, C. Madic and M. Ephritikhine, *J. Chem. Soc., Dalton Trans.*, 2002, 3265.
23 P. B. Iveson, C. Riviere, D. Guillaneux, M. Nierlich, P. Thuéry, M. Ephritikhine and C. Madic, *Chem. Commun.*, 2001, 1512.
24 C. Madic, M. Lecomte, P. Baron and B. Boulis, *C. R. Phys.*, 2002, **3**, 797–811.
25 J. Polin, E. Schmohel and V. Balzani, *Synthesis*, 1998, **3**, 321–324.
26 T. Norrby, A. Boerje, L. Zhang and B. Akermark, *Acta Chem. Scand.*, 1998, **52**, 77–85.
27 B. J. Childs, D. C. Craig, M. L. Scudder and H. A. Goodwin, *Aust. J. Chem.*, 1998, **51**, 895.
28 F. H. Case, *J. Heterocycl. Chem.*, 1971, **8**, 173.
29 W. Kabsch, *J. Appl. Crystallogr.*, 1988, **21**, 916.
30 Shelx86, G. M. Sheldrick, *Acta Crystallogr., Sect. A*, 1990, **46**, 467.
31 N. Walker and D. Stuart, *Acta Crystallogr., Sect. A*, 1983, **39**, 158.
32 Shelxl, G. M. Sheldrick, Program for crystal structure refinement, University of Göttingen, Germany, 1993.
33 D. F. Evans and C. Y. Wong, *J. Chem. Soc., Dalton Trans.*, 1992, 2009.
34 M. Shamsipur and A. I. Popov, *Inorg. Chim. Acta*, 1980, **43**, 243.
35 C. Srivanavit, J. I. Zink and J. J. Dechter, *J. Am. Chem. Soc.*, 1977, **99**, 5876.
36 H. Suzuki and T. Mori, *J. Chem Soc., Perkin Trans. 1*, 1995, 291.
37 M. G. B. Drew, D. Guillaneux, M. J. Hudson, P. B. Iveson and C. Madic, *Inorg. Chem. Commun.*, 2001, **4**, 462.
38 M. S. Grigoriev, C. Den Auwer and C. Madic, *Acta Crystallogr., Sect. C*, 2001, **57**, 1141.
39 S. Wang, Y. Zhu, Y. Cui, L. Wang and Q. Luo, *J. Chem. Soc., Dalton Trans.*, 1994, 2523.
40 G. Y. S. Chan, M. G. B. Drew, M. J. Hudson, N. S. Isaacs, P. Byers and C. Madic, *Polyhedron*, 1996, **15**, 3385.
41 F. H. Allen and O. Kennard, *Chem. Des. Automat. News*, 1993, **8**, 31.
42 D. A. Fletcher, R. F. McMeeking and D. Parkin, *J. Chem. Inf. Comput. Sci.*, 1996, **36**, 746.
43 M. J. Plater, M. R. S. Foreman, R. A. Howie, J. M. S. Skakle, E. Coronado, C. J. Gomez-Garcia, T. Gelbrich and M. B. Hursthouse, *Inorg. Chim. Acta*, 2001, **319**, 159.
44 P. C. Leverd, M. C-. Charbonnel, J.-P. Dognon, M. Lance and M. Nierlich, *Acta. Crystallogr., Sect. C*, 1999, **55**, 368.
45 M. R. S. Foreman, M. J. Plater and J. M. S. Skakle, *J. Chem. Soc., Dalton Trans.*, 2001, 1897.
46 C. S. Bruschini, M. G. B. Drew, M. J. Hudson and K. Lyssenko, *Polyhedron*, 1995, **14**, 3099.
47 F. A. Cotton and P. R. Raithby, *Inorg. Chem. Commun.*, 1999, **2**, 86.
48 A. K. Boudalis, V. Nastopoulos, A. Terzis, C. P. Raptopoulou and S. P. Perlepes, *Z. Naturforsch., Teil B*, 2001, **56**, 122.

49 G. Ionova, C. Rabbe, R. Guillaumont, S. Ionov, C. Madic, J.-C. Krupa and D. Guillaneux, *New J. Chem.*, 2002, **26**, 234.
50 M. J. Frisch, G. W. Trucks, H. B. Schlegel, G. E. Scuseria, M. A. Robb, J. R. Cheeseman, V. G. Zakrzewski, J. A. Montogomery, R. E. Stratman, J. C. Burant, S. Dapprich, J. M. Millam, A. D. Daniels, K. N. Kudin, M. C. Strain, O. Farkas, J. Tomasi, V. Barone, M. Cossi, R. Cammi, B. Mennucci, C. Pomelli, C. Adamo, S. Clifford, J. Ochterski, G. A. Petersson, P. Y. Ayala, Q. Cui, K. Morokuma, D. K. Malick, A. D. Rabuck, K. Raghavachari, J. B. Foresman, J. Cioslowski, J. V. Ortiz, B. B. Stefanov, G. Liu, A. Liashenko, P. Piskorz, I. Komaromi, R. Gomperts, R. L. Martin, D. J. Fox, T. Keith, M. A. Al-Latham, C. Y. Peng, A. Nanayakkara, C. Gonzalez, M. Challacombe, P. M. W. Gill, B. Johnson, W. Chen, M. W. Wong, J. L. Andres, M. Head-Gordon, E. S. Replogle, J. A. Pople, Gaussian98 program, Gaussian, Inc., Pittsburgh, PA, 1998.